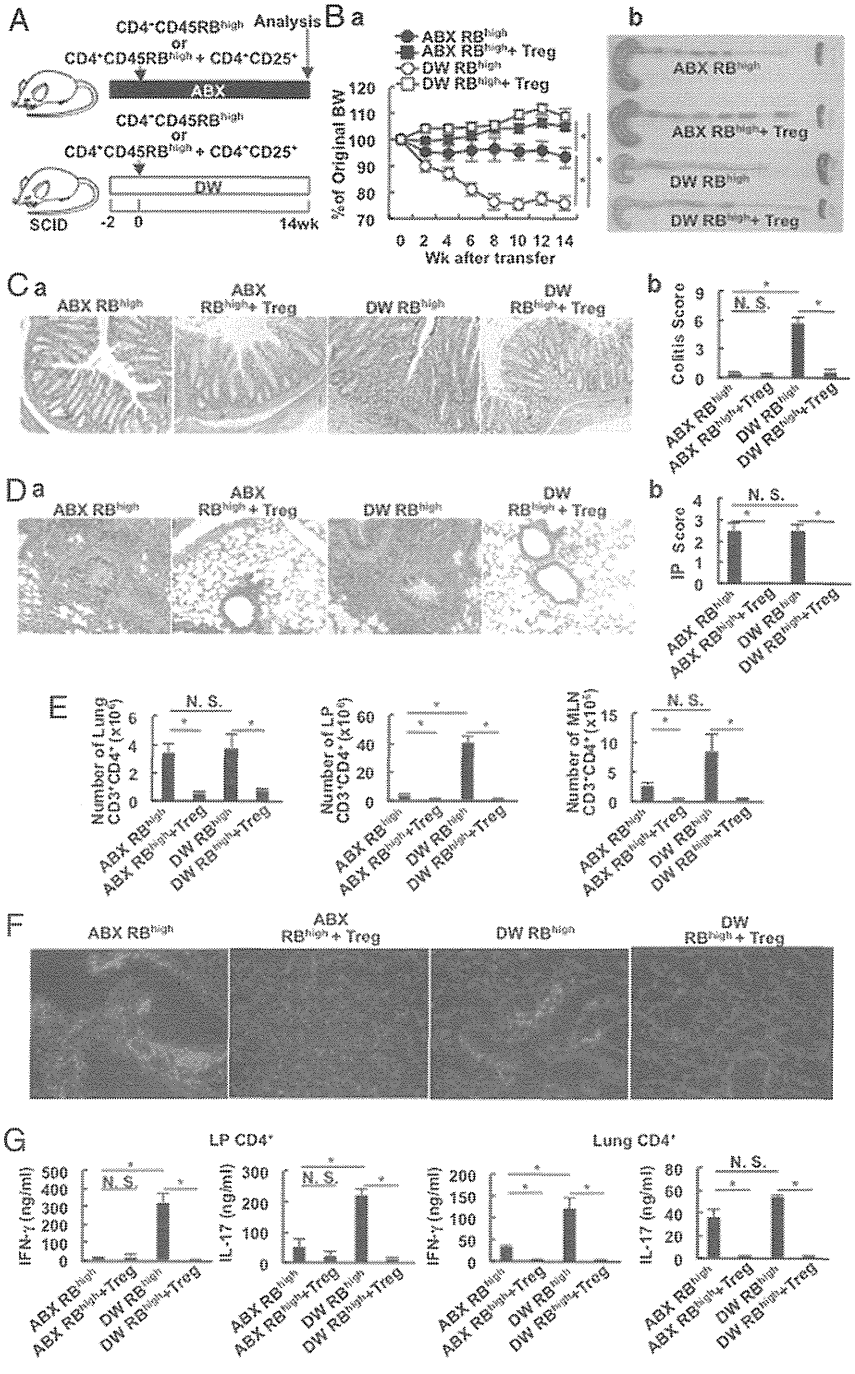

FIGURE 1. Antibiotic treatment prevents the development of colitis, but not pneumonitis. (**A**) Two weeks before transfer, two groups (ABX RB^{high} and ABX RB^{high} + Treg) of CB17-icr SCID mice were pretreated with a combination of antibiotics, whereas the other two groups (DW RB^{high} and DW RB^{high} + Treg) were given distilled water. The same number of $CD4^+$ $CD45RB^{high}$ T cells was transferred into each mouse, with mice in the ABX RB^{high} + Treg and DW RB^{high} + Treg groups receiving the same number of $CD4^+CD25^+$ Treg. Ten weeks later, the mice were sacrificed and analyzed. (**Ba**) Time course of percentage of original body weight. Data are shown as the mean ± SEM for five mice per group. $*p < 0.01$. (**Bb**) Gross appearance of the colon, MLN, and SP from mice in each group at sacrifice. (**Ca**) Histopathology of the distal colon of the indicated mice 10 wk after transfer. Original magnification ×100. (**Cb**) Histological scores. Data are shown as the mean ± SEM for five mice per group. $*p < 0.01$. (**Da**) Histopathology of the lung of the indicated mice 10 wk after transfer. Original magnification ×100. (**Db**) IP scores. Data are shown as the mean ± SEM for five mice per group. $*p < 0.01$. (**E**) Absolute numbers of $CD3^+CD4^+$ cells in the lung, colonic LP, and MLN 10 wk after transfer. Data are shown as the mean ± SEM. $*p < 0.01$. (**F**) Expression of CD4 in frozen lung sections from each group 10 wk after transfer. Red indicates CD4; blue indicates DAPI. Original magnification ×200. (**G**) Cytokine production by lung and LP $CD4^+$ T cells isolated 10 wk after transfer and stimulated in vitro. IFN-γ and IL-17 concentrations in culture supernatants were measured by ELISA. Data are shown as the mean ± SEM for five mice per group. $*p < 0.05$.

$CD4^+$ T cells, respectively (Fig. 2A), with responses to CBA being dose dependent. Although colitic lung $CD4^+$ T cells produced significantly less IFN-γ than colitic LP $CD4^+$ T cells upon stimulation by the same concentration of CBA, the two cell types produced comparable levels of IL-17A in response to CBA (Fig. 2A). These results indicated that colitic lung $CD4^+$ T cells can respond to intestinal bacterial Ags and may therefore be colitogenic, like colitogenic LP $CD4^+$ T cells. To determine whether lung $CD4^+$ T_{EM} cells generated in ABX-treated mice can respond to intestinal bacterial Ags, lung and LP $CD4^+$ T cells of ABX-treated and DW-treated SCID mice injected with $CD4^+CD45RB^{high}$ T cells were cocultured with CBA-pulsed APC. Surprisingly, lung $CD4^+$ T cells from ABX-treated mice produced very small amounts of IL-17 and IFN-γ in response to CBA (Fig. 2B) while producing larger amounts both in response to anti-CD3/CD28 Abs (Fig. 1G). This result suggested that most lung $CD4^+$ T cells in ABX-treated mice were not "intestinal microbiota–reactive T_{EM} cells."

IP occurs independent of Th17

Consistent with our finding that colitic lung $CD4^+$ T_{EM} cells preferentially produce IL-17 rather than IFN-γ in response to CBA (Fig. 2A), a recent study suggested that lung IL-17-producing $CD4^+$ T cells, including Th17 cells, are critically involved in inducible BALTs during acute influenza virus infection of mice (13). We therefore hypothesized that colitogenic RORγ*t*-dependent Th17 cells, rather than colitogenic Th1 cells, are involved in the development of IP in this transfer model. To assess this, we isolated colitogenic $CD3^+CD4^+RORγt^+$ (GFP^+) and $RORγt^-$ (GFP^-) cells from the colons of colitic RAG-$2^{-/-}$ mice previously injected

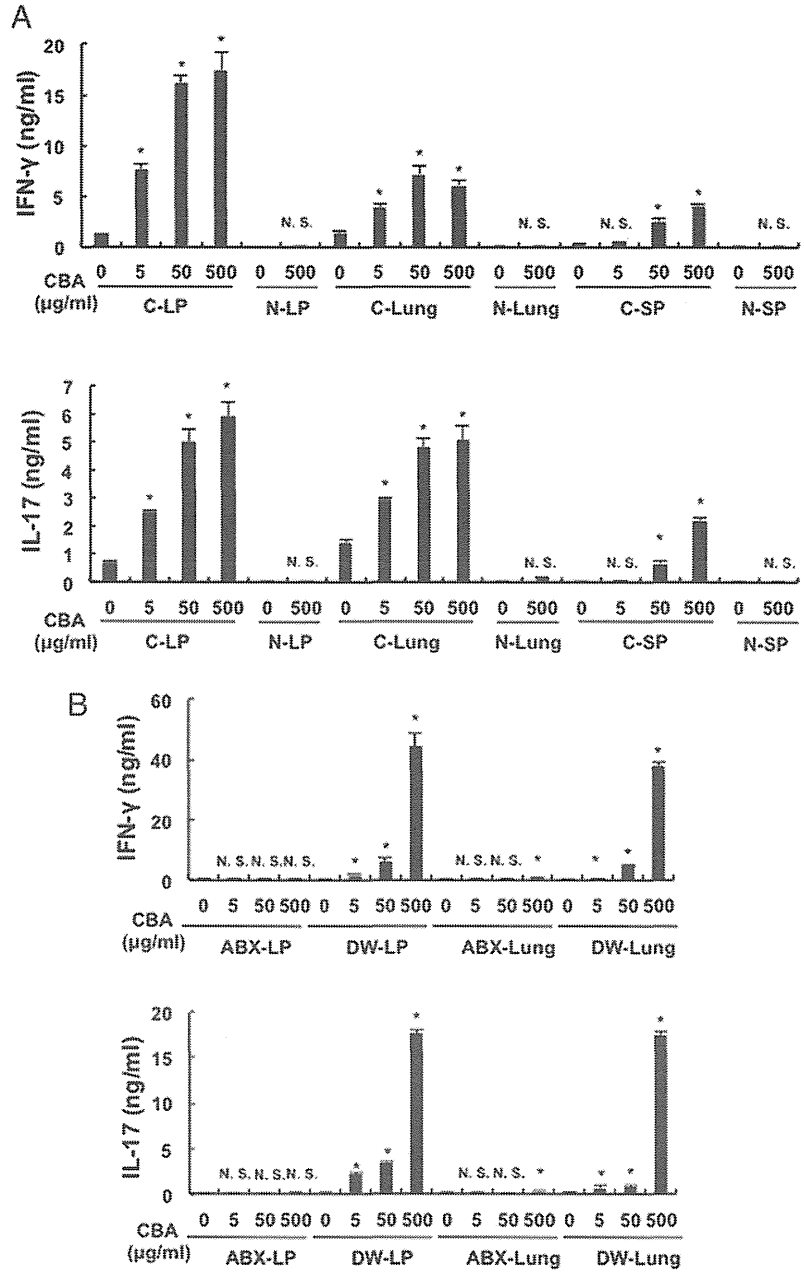

FIGURE 2. $CD4^+$ T cells in the lungs of colitic mice respond to cecal Ags. (**A**) Cytokine production by lung, LP and SP $CD4^+$ T cells from colitic and normal mice. Lung, LP and SP $CD4^+$ T cells were isolated and stimulated with various concentrations of CBA-pulsed APC in vitro. IFN-γ and IL-17 concentrations in culture supernatants were measured by ELISA. Data are shown as the mean ± SEM for five wells per group. (**B**) SCID mice were pretreated with ABX or DW, followed by transfer of $CD4^+CD45RB^{high}$ T cells. Six weeks later, the lung and LP $CD4^+$ T cells in both groups were isolated and stimulated in vitro with various concentrations of CBA-pulsed APC. IFN-γ and IL-17 concentrations in culture supernatants were measured by ELISA. Data are shown as the mean ± SEM for three wells per group. $*p < 0.05$ compared with negative control, 0 μg/ml CBA.

with $CD4^+CD45RB^{high}$ T cells from RORγ*t*-GFP reporter mice and then retransferred colitogenic GFP^+ or GFP^- cells to new RAG-$2^{-/-}$ mice ($ROR\gamma t^+$ and $ROR\gamma t^-$ mice, respectively). The $ROR\gamma t^+$ T cells were a mixture of IL-$17^-IFN\gamma^+$, IL-$17^+IFN\gamma^-$, and IL-$17^+IFN\gamma^+$ cells, whereas most $ROR\gamma t^-$ T cells are IL-$17^-IFN\gamma^+$, because $ROR\gamma t^+IFN\gamma^-$IL-17^+ Th17 cells differentiate to $ROR\gamma t^+IFN\gamma^+$IL-17^- "alternative Th1" cells (14). As positive and negative controls, RAG-$2^{-/-}$ mice were transferred with whole colitic LP $CD3^+CD4^+$ cells with or without splenic $CD4^+CD25^+$ T_R cells (colitic $CD4^+$ and $CD4^+ + T_R$ mice, respectively). We also assessed the dominance of $ROR\gamma t^+$ and $ROR\gamma t^-$ cells in the lungs when these cells were transferred with whole colitogenic $CD3^+$ $CD4^+$ cells by evaluating GFP expression (Fig. 3A). $ROR\gamma t^+$, $ROR\gamma t^-$, and colitic $CD4^+$ mice developed severe colitis, whereas colitic $CD4^+$ + Treg mice did not (Fig. 3A). The histological scores of $ROR\gamma t^+$, $ROR\gamma t^-$, and colitic $CD4^+$ mice were comparable but were significantly higher the scores of colitic $CD4^+ + T_R$ mice (Fig. 3C). Large numbers of mononuclear cells infiltrated the lung interstitial areas of $ROR\gamma t^+$, $ROR\gamma t^-$, and colitic $CD4^+$ mice, with small numbers of cells found in the same area in colitic $CD4^+ + T_R$ mice (Fig. 3D). In addition, IP scores in $ROR\gamma t^+$, $ROR\gamma t^-$, and colitic $CD4^+$ mice were comparable and significantly higher than in colitic $CD4^+ + T_R$ mice (Fig. 3E). The numbers of $CD3^+CD4^+$ cells in the lungs and colonic LP were comparable in $ROR\gamma t^+$, $ROR\gamma t^-$, and colitic $CD4^+$ mice, with all three being significantly higher the numbers in colitic $CD4^+ + T_R$ mice (Fig. 3F). We also assessed the proportion of GFP^+ cells in the lungs, colonic LP, MLN, and SP of the four groups. There were almost no GFP^+ cells in any organ of $ROR\gamma t^-$ mice, whereas one-half to one-third of GFP^+ cells were lost in the organs of $ROR\gamma t^+$ mice (Supplemental Fig. 3A), suggesting in vivo conversion from Th17 cells to alternative Th1 cells, as previously shown by our group (14). Almost no IL-17–producing cells were present in the lungs and LP of $ROR\gamma t^-$ mice, with higher proportions in the organs of the other groups, and no difference in the number of IFN-γ–producing cells in the $ROR\gamma t^+$, $ROR\gamma t^-$, and $CD4^+$ groups (Supplemental Fig.

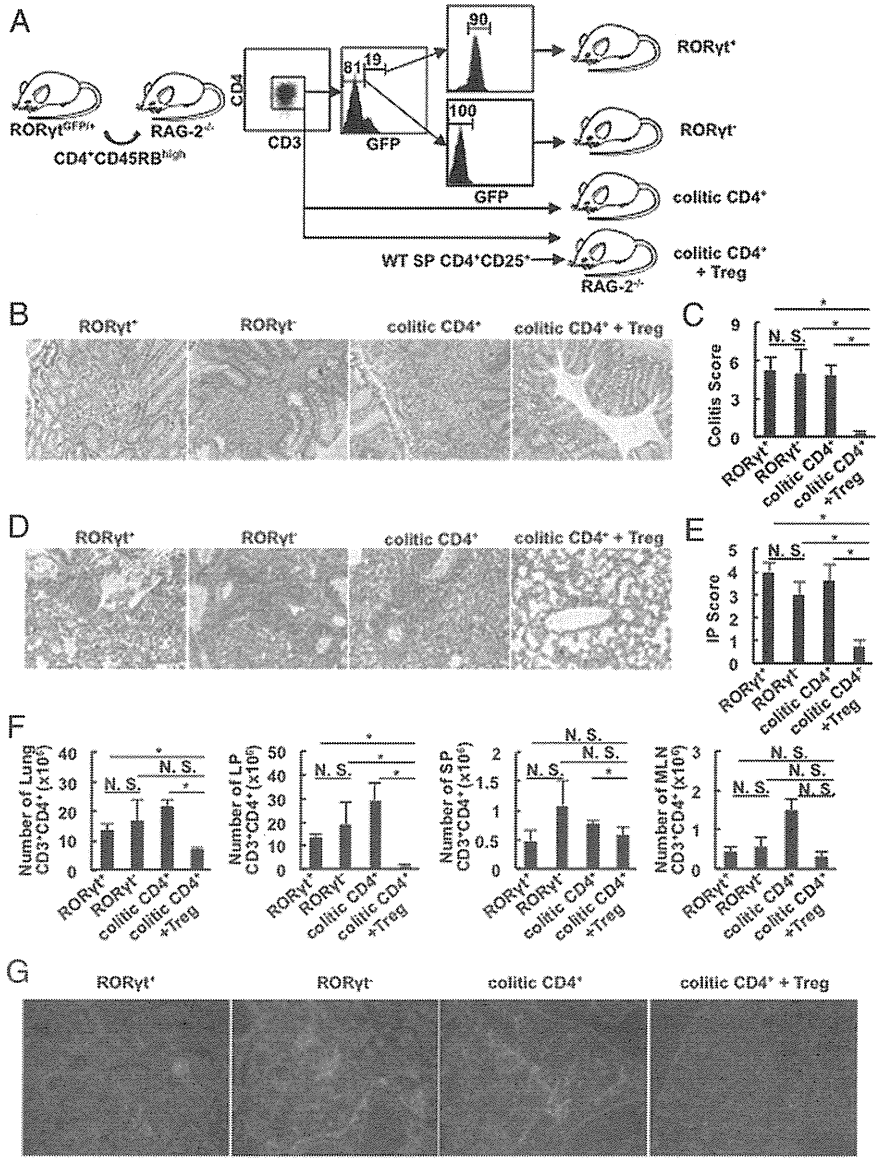

FIGURE 3. Colitogenic Th1 and Th17 cells have comparable abilities to induce pneumonitis . (**A**) Colitogenic $CD3^+CD4^+ROR\gamma t^+$ and $ROR\gamma t^-$ cells were isolated from colitic RAG-$2^{-/-}$ mice previously injected with $CD4^+CD45RB^{high}$ T cells from RORγ*t*-GFP reporter mice, and each was retransferred to new RAG-$2^{-/-}$ mice ($ROR\gamma t^+$, $ROR\gamma t^-$). As a positive control, RAG-$2^{-/-}$ mice were injected with whole colitogenic $CD3^+CD4^+$ cells from colitic RAG-$2^{-/-}$ mice ($CD4^+$). As a negative control, RAG-$2^{-/-}$ mice were injected with whole colitogenic $CD3^+CD4^+$ cells from colitic RAG-$2^{-/-}$ mice and splenic $CD4^+CD25^+$ T cells from normal mice ($CD4^+ + T_R$). (**B**) Histopathology of the distal colon of the indicated mice 10 wk after the retransfer. Original magnification ×100. (**C**) Histological scores. Data are shown as the mean ± SEM for four mice per group. (**D**) Histopathology of the lungs of the indicated mice 10 wk after transfer. Original magnification ×100. (**E**) IP scores. Data are shown as the mean ± SEM for four mice per group. (**F**) Absolute number of $CD3^+CD4^+$ cells in the lung, colonic LP, SP, and MLN 10 wk after retransfer. Data are shown as the mean ± SEM. (**G**) Expression of CD4 by frozen sections of lung from each group. Tissue samples obtained 10 wk after the retransfer were incubated with anti-CD4 Abs. Red indicates CD4; blue indicates DAPI. Original magnification ×200. $*p < 0.01$.

3B). Immunohistochemistry showed that most of the mononuclear cells infiltrating the lung interstitial lesions of these three groups were $CD4^+$ T cells (Fig. 3G).

Colitogenic $CD4^+$ T_{EM} cells in the colon and lungs share similar expression patterns of gut- and lung-homing receptors

To evaluate the possible developmental correlation between colitis and pneumonitis in this transfer model, we assessed the expression of homing receptors on lung and LP $CD3^+CD4^+$ T cells in colitic SCID mice previously injected with $CD4^+CD45RB^{high}$ T cells, with normal BALB/c mice as the negative control. Colonic LP and lung $CD3^+CD4^+$ T cells in colitic mice expressed integrin $\alpha_4\beta_7$ and CCR6, both homing receptors for the intestine, but did not express CCR7, a homing receptor for the lymph node. Surprisingly, colitic LP $CD3^+CD4^+$ cells expressed a higher level of CD49a, a homing receptor for lung (15, 16), than colitic lung $CD3^+CD4^+$ cells (Fig. 4). We also assessed the expression of homing receptors on $CD3^+CD4^+$ T cells from each organ of colitic IL-$2^{-/-}$ and normal C57BL/6J mice as negative controls. Lung and LP $CD3^+CD4^+$ T cells in colitic IL-$2^{-/-}$ mice expressed high levels of CCR6 and CD49a but low levels of CCR7 (data not shown).

Lung $CD4^+$ T cells of SCID mice injected with $CD4^+$ $CD45RB^{high}$ T cells preferably migrate to the lungs

We also assessed whether colitic lung and LP $CD4^+$ T cells, which express high levels receptors for homing to the lungs and intestine, can migrate to the lung and LP after transfer into new SCID mice. Both lung $CD4^+$ T cells and LP $CD4^+$ T cells from colitic SCID mice were transferred into new SCID mice (Supplemental Fig. 4A), sacrificed 3 wk later, and analyzed. Interestingly, larger numbers of lung than of LP $CD4^+$ T cells migrated to the lungs, whereas almost the same number of both migrated to LPs, MLNs and SPs (Supplemental Fig. 4B).

Lung $CD4^+$ T cells of SCID mice injected with $CD4^+$ $CD45RB^{high}$ T cells and treated with ABX have the potential to induce colitis

We next examined whether colitic lung $CD4^+$ T cells have the potential to induce pneumonitis and/or colitis if transferred to new SCID mice with or without ABX treatment (Fig. 5A). As expected, colitis developed only in SCID mice injected with $CD4^+$ T cells from the lungs of ABX RB^{high} mice without (DW Lung Re-Tr mice) not with (ABX Lung Re-Tr mice) subsequent ABX treatment (Fig. 5B, 5C). Furthermore, significantly fewer LP cells

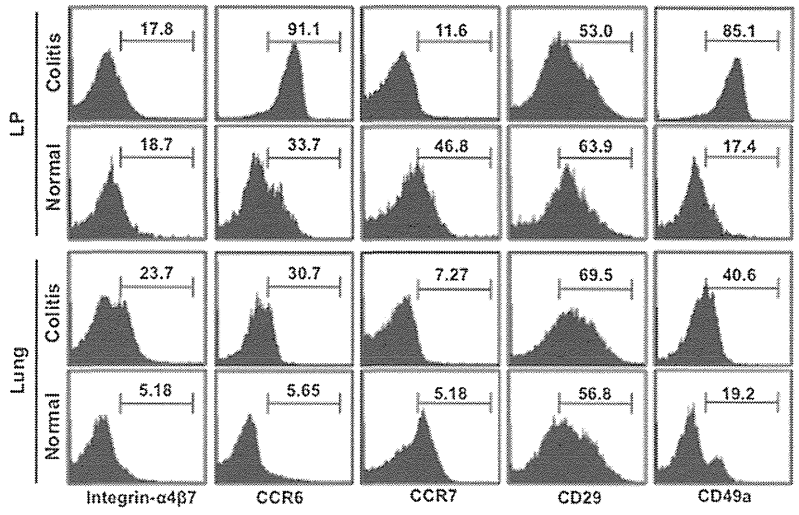

FIGURE 4. Expression of various homing receptors on $CD4^+$ T cells in organs from colitic mice. LP and lung $CD3^+CD4^+$ T cells were isolated from colitic SCID mice previously injected with $CD4^+CD45RB^{high}$ T cells and from normal BALB/c mice, and the expression of various homing receptors on $CD3^+CD4^+$ gated cells was determined by flow cytometry. Representative results of five samples per group. The numbers in the plots indicate the mean of five mice per group.

were recovered from ABX Lung Re-Tr than DW Lung Re-Tr mice (Fig. 5D), whereas both groups developed pneumonitis ~6 wk after retransfer (Fig. 5E) with comparable IP scores (Fig. 5F) and numbers of recovered lung $CD3^+CD4^+$ T cells (Fig. 5G), suggesting that pneumonitis is induced independently of the presence of living intestinal microbiota.

Intestinal microbiota are not essential for the development of pneumonitis in SCID mice injected with $CD4^+CD45RB^{high}$ T cells

To exclude the possibility that lung harbor bacteria may cause IP, even after ABX treatment, we used a GF system to completely exclude the possible contribution of living bacteria in the intestine or in the lung from inhalation. Again, we found that SCID mice injected with $CD4^+CD45RB^{high}$ T cells under SPF conditions (SPF RB^{high} mice) developed severe colitis and IP 6 wk later, whereas SCID mice injected with $CD4^+CD45RB^{high}$ T cells under GF conditions (GF RB^{high} mice) developed IP but not colitis (Fig. 6A, 6C). The colitis and IP scores of these two groups provided statistical confirmation (Fig. 6B, 6D). When lung $CD3^+CD4^+$ T cells isolated from GF RB^{high} mice were retransferred to new SPF (SPF Lung Re-Tr mice) or GF SCID (GF Lung Re-Tr mice) mice (Fig. 6E), the former group developed pneumonitis and colitis, whereas the latter developed pneumonitis but not colitis (Fig. 6F, 6H), similar to the ABX treatment system. These observations were also confirmed by statistical analysis (Fig. 6G, 6I).

$CD4^+CD45RB^{high}$ T cells of GF donor mice also induce IP

We thought that the TCR repertoires of naive T cells may differ in GF donors, in which all intestinal bacteria-reactive T cells remain naive, and SPF donors, in which some intestinal bacteria-reactive T cells, have already become memory T cells. We also assessed whether $CD4^+CD45RB^{high}$ T cells from GF donor mice can induce colitis upon transfer to new SCID mice, with or without ABX treatment (Fig. 7A). We found that these GF $CD4^+CD45RB^{high}$ T cells could induce Th1/Th17-mediated colitis and pneumonitis (Fig. 7B–I). The expression of CD49a and integrin $\alpha_4\beta_7$ by lung $CD3^+CD4^+$ T cells was slightly lower in ABX-treated than in DW-treated mice (Fig. 7J). Lung and LP $CD4^+$ T cells generated from GF donor mice in DW-treated SCID mice produced large amount of IL-17 and IFN-γ in response to CBA in vitro, whereas cells in ABX-treated SCID mice produced very small amounts of IL-17 and IFNγ (data not shown).

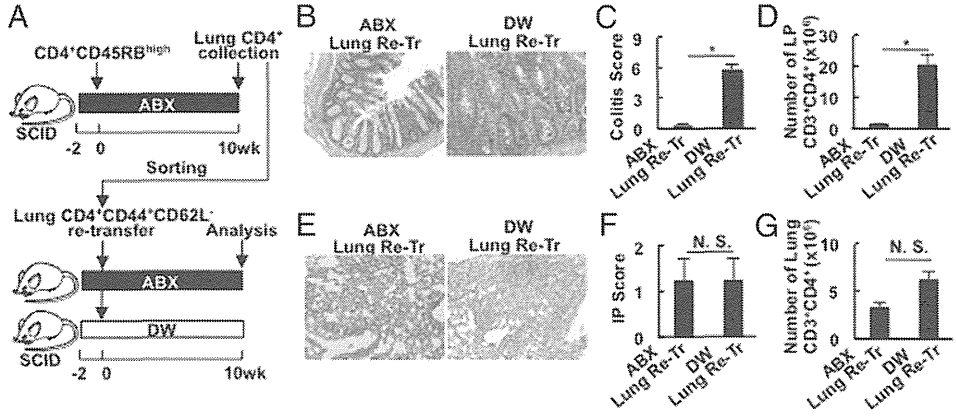

FIGURE 5. Lung $CD4^+$ T_{EM} can induce both IP and colitis. (**A**) CB17-icr SCID mice were pretreated with the combination of antibiotics for 2 wk and injected with the same number of $CD4^+CD45RB^{high}$ T cells. Ten weeks later, the mice were sacrificed, and their lung $CD4^+$ T cells were isolated. The $CD3^+CD4^+CD44^+CD62L^-$ population was sorted and reinjected into new SCID mice pretreated with ABX (ABX Lung Re-Tr) or distilled water (DW Lung Re-Tr). (**B**) Histopathology of the distal colons of the indicated mice 10 wk after retransfer. (**C**) Histological scores. Data are shown as the mean ± SEM for three mice per group. (**D**) Absolute number of $CD3^+CD4^+$ cells in colonic LP. Data are shown as mean ± SEM. (**E**) Histopathology of lung of the indicated mice 10 wk after retransfer. (**F**) IP scores. Data are shown as the mean ± SEM for three mice per group. (**G**) Absolute number of $CD3^+CD4^+$ T cells in lung. Data are shown as mean ± SEM. Original magnification ×100. $*p < 0.01$.

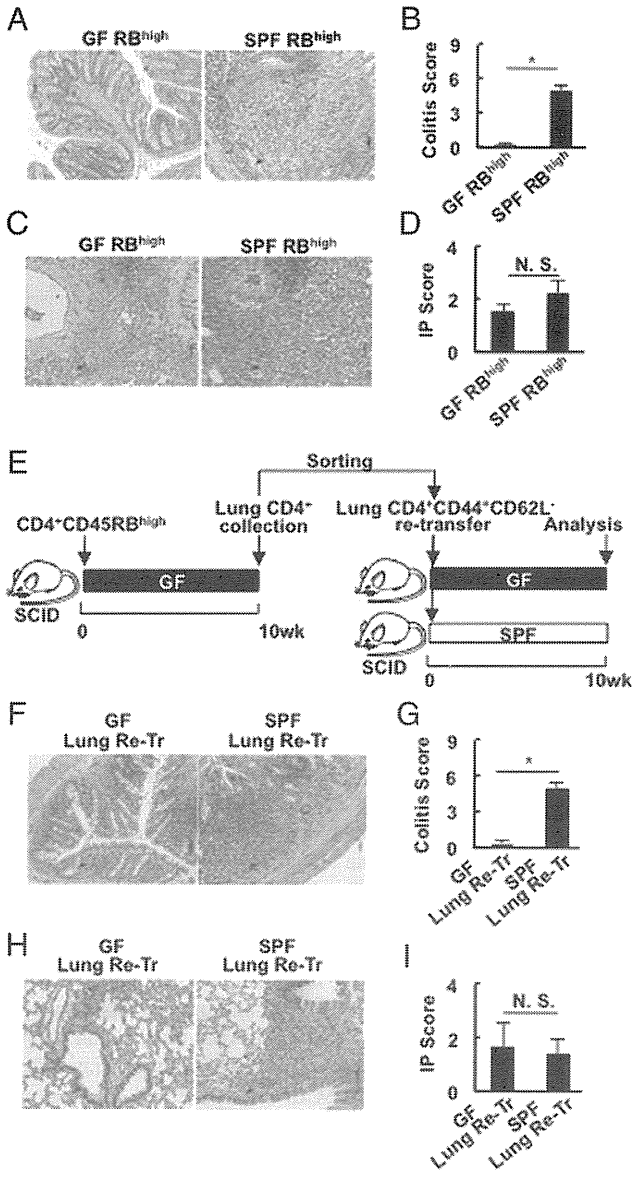

FIGURE 6. Commensal bacteria are not essential for the development of IP. (**A–D**) GF or SPF C3HeJ SCID mice were injected with $CD4^+$ $CD45RB^{high}$ T cells. (A) Histopathology of the distal colon of the indicated mice 10 wk after transfer. (B) Histological scores. Data are shown as the mean ± SEM for eight GF and four SPF mice. (C) Histopathology of the lungs of the indicated mice 10 wk after transfer. (D) IP scores. Data are shown as the mean ± SEM for eight GF and four SPF mice. (**E**) GF C3HeJ SCID mice were injected with $CD4^+CD45RB^{high}$ T cells and sacrificed 10 wk later. Lung $CD4^+$ T cells were isolated, and $CD3^+CD4^+CD44^+CD62L^-$ cells were sorted with FACSAria II and injected into new GF (GF Lung Re-Tr) or SPF (SPF Lung Re-Tr) C3HeJ SCID mice. (**F**) Histopathology of the distal colon of the indicated mice 10 wk after retransfer. (**G**) Histological scores. Data are shown as the mean ± SEM for three mice per group. (**H**) Histopathology of the lungs of the indicated mice 10 wk after retransfer. Original magnification ×100. (**I**) IP scores. Data are shown as the mean ± SEM for three mice per group. Original magnification ×100. $^*p < 0.01$.

Discussion

We have shown in this study that living intestinal microbiota are required for the development of intestinal, but not lung, inflammation in an adoptive transfer model of colitis. Furthermore, we showed that infiltrating lung $CD4^+$ T_{EM} cells generated under ABX-treated or GF conditions have the potential to induce colitis if transferred under SPF conditions. These surprising findings clearly indicate that intestinal microbiota are essential for the development of intestinal, but not lung, inflammation, at least during lymphopenia-driven cell expansion.

In assessing the mechanisms that mediate the development of lung inflammation in ABX-treated mice under GF conditions, it was surprising to find that chronic inflammation in GF SCID mice injected with $CD4^+CD45RB^{high}$ T cells occurs only in lung but not in any other tissue examined. Over 90% of SPF SCID mice injected with $CD4^+CD45RB^{high}$ T cells develop colitis, with 84, 44, 26, and < 10% also developing low levels of inflammation of the stomach, liver, lungs, and other tissues, respectively (17). Differences in level of inflammation may be due to the use of immune-deficient recipient mice obtained from different animal facilities or to environmental factors that drive the inflammatory response, because the nature of the endogenous microbiota in immune-deficient recipients may be important and may vary among facilities. Although GF SCID mice injected with $CD4^+$ $CD45RB^{high}$ T cells do not develop colitis, the absence of inflammation in other tissues under GF conditions has not been experimentally established. Because we found that SPF SCID mice injected with $CD4^+CD45RB^{high}$ T cells developed both colitis and IP, we initially hypothesized that colitogenic $CD4^+$ T_{EM} cells were originally generated in response to intestinal bacterial Ags presented by professional APCs at intestinal sites, subsequently migrating to the lungs to establish lung inflammation. It was unclear, however, how aberrantly migrating $CD4^+$ T_{EM} cells could be maintained in the lungs. Surprisingly, however, we found that GF- and ABX-treated SCID injected with $CD4^+CD45RB^{high}$ T cells developed IP with infiltration of $CD4^+$ T_{EM} cells but did not develop colitis. These T_{EM} cells may not just be retained in the lungs but may be pathogenic because lung $CD4^+$ T cells from ABX-treated SCID mice produced large amount of IFN-γ and IL-17 in response to anti-CD3/CD28 stimulation but produced very small amounts of IL-17 and IFN-γ in response to CBA in vitro. These results suggested that most lung $CD4^+$ T cells in ABX-treated mice were not "intestinal microbiota–reactive T_{EM} cells," but became intestinal microbiota–reactive T_{EM} cells upon injection into SPF SCID mice. This result suggests that, in GF- and ABX-treated mice, $CD4^+$ T cells expand in the lungs in response to self-Ags. Because these cells produced very small amounts of IFN-γ and IL-17 in response to intestinal bacterial Ags, some may have cross-reactivity to intestinal Ags. Upon transfer into new SCID mice under SPF conditions, the cell population reactive to intestinal bacteria expands and induces colitis. Because these "colitogenic" $CD4^+$ T cells were generated in the lungs, they have homing receptors to the lungs. Finally, these cells migrate to the lungs, where they also induce interstitial pneumonitis. Another hypothesis is that lung $CD4^+CD44^+CD62L^-$ "T_{EM}-like" cells generated in ABX-treated mice were not "effector" or "memory" cells but had a "memory-like" phenotype generated through homeostatic expansion in lymphopenic hosts (18). Upon injection into ABX-treated GF SCID mice, these naive $CD4^+$ T cells expand in the lungs in the absence of cognate Ag activation, making them memory–phenotype (MP) cells. Injection of these MP cells into new SCID mice under SPF conditions results in the expansion of MP cells specific to intestinal bacterial Ags, thus inducing colitis.

Although athymic BALB/c nude mice reconstituted with $CD4^+$ $CD25^-$ T_R cells spontaneously develop histologically and serologically evident autoimmune diseases, such as thyroiditis, gastritis, insulitis, sialoadenitis, adrenalitis, oophoritis, glomerulonephritis, and polyarthritis, but not colitis or pneumonitis, under SPF conditions (19, 20), it is not known whether they develop these diseases

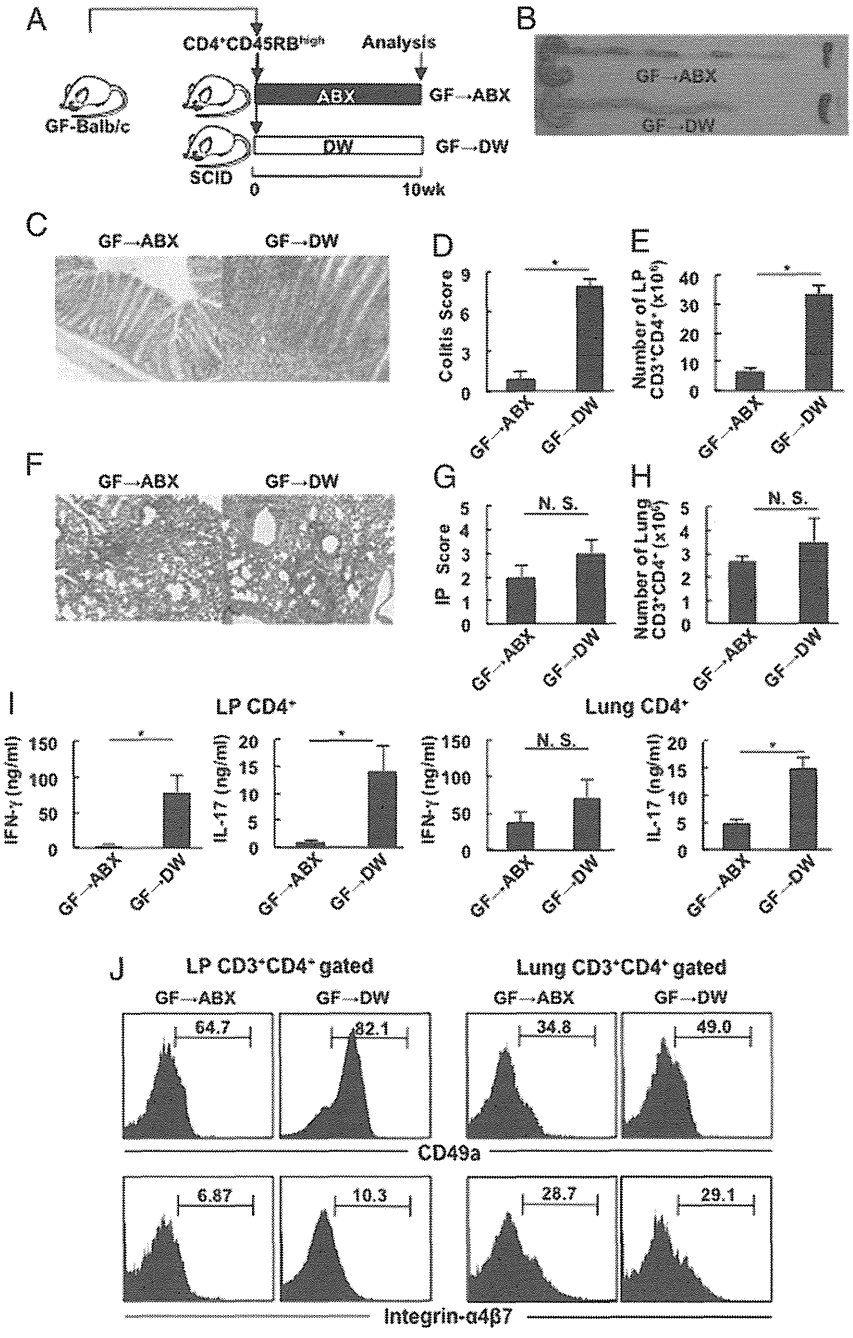

FIGURE 7. $CD4^+CD45RB^{high}$ T cells from GF donor also induced both colitis and IP. (**A**) Two weeks before the transfer, one group of CB17-icr SCID mice were pretreated with the combination of antibiotics (GF→ABX), whereas the other group were given distilled water (GF→DW). Then the same number of $CD4^+$ $CD45RB^{high}$ T cells isolated from GF BALB/c mice were transferred to each group. Ten weeks after the transfer, all mice were sacrificed and analyzed. (**B**) Gross appearance of the colon, MLN, and SP from mice of each group at 10 wk after the transfer. (**C**) Histopathology of distal colon of the indicated mice 10 wk after the transfer. (**D**) Histological scores. Data are shown as the mean ± SEM for five mice in each group. $*p < 0.01$. (**E**) Absolute $CD3^+CD4^+$ cell number of LP. Data are shown as the mean ± SEM. $*p < 0.01$. (**F**) Histopathology of lung of the indicated mice 10 wk after the transfer. (**G**) IP scores. Data are shown as the mean ± SEM for five mice in each group. (**H**) Absolute $CD3^+CD4^+$ cell number of LP. Data are shown as the mean ± SEM. (**I**) Cytokine production by lung and LP $CD4^+$ T cells. Lung and LP $CD4^+$ T cells were isolated 10 wk after the transfer and stimulated in vitro. IFN-γ and IL-17 concentrations in culture supernatants were measured by ELISA. Data are shown as the mean ± SEM for five mice in each group. $*p < 0.05$. (**J**) Expression of CD49a and integrin $\alpha_4\beta_7$ on $CD3^+CD4^+$ gated cells in the LP and lung of each group. Representative results of five samples in each group. Numbers in the plots indicate the mean of five mice in each group. Original magnification ×100.

under GF conditions. Even if GF nude mice injected with $CD4^+$ $CD25^-$ T cells develop IP or other autoimmune diseases, a different mechanism appears to underlie the development of IP in GF SCID mice injected with $CD4^+CD45RB^{high}$ T cells. First, the nude transfer autoimmune model requires a large enough number of donor $CD4^+CD25^-$ T cells (2×10^6–1×10^7 cells/mouse) to block lymphopenia-driven T cell expansion, compared with the lower number of donor $CD4^+CD45RB^{high}$ T cells (~3–4 × 10^5 cells/mouse) in the SCID/RAG-$1/2^{-/-}$ transfer colitis model. Consistent with this, RAG-$1^{-/-}$ mice with over 1×10^7 $CD4^+CD45RB^{high}$ T cells did not develop colitis, even under SPF conditions, owing to the lack of lymphopenia-driven T cell expansion (21). Moreover, autoantigen-reactive $CD4^+CD25^-$ T_{EM} cells in the $CD4^+CD45RB^{low}$ subpopulation may expand slowly (22). Consistent with this finding, the period required to establish disease is longer for the nude transfer (over 15 wk) than for the SCID/RAG-$1/2^{-/-}$ transfer (~6–8 wk) colitis model. These findings indicate that our model of microbiota-reactive T cell–mediated pneumonitis in the absence of microbiota (GF) or in the presence of small numbers (ABX treatment) is a unique and valuable tool to investigate the immunological mechanisms of extraintestinal disorders in patients with IBD.

From a clinical perspective, although pulmonary diseases are thought to be rare in IBD patients, prospective studies have suggested that a significant proportion of these patients have complicating pulmonary diseases, including chronic bronchitis, bronchiectasis, bronchiolitis obliterans with organizing pneumonia, and parenchymal nodules (23). Our model seems to be similar to bronchiolitis obliterans with organizing pneumonia, a typical interstitial lung disorder. Although the manifestations of pulmonary disease usually parallel intestinal disease activity, as seen in our model under SPF conditions, our model suggests that pulmonary lesions may be maintained, at least at an immunological level, even after intestinal

remission and act as a reservoir of microbiota-reactive T_{EM} cells that can cause recurrence. Consistent with this, we showed that adoptive transfer of T_{EM} cells from ABX-treated or GF mice into SPF recipient mice reproduces colitis comparable with the original colitis in this model. Further studies are required on a range of clinical issues, such as recent overuse of ABX and the increased incidence of autoimmune diseases due to excessive hygiene.

In summary, we have established a unique microbiota-reactive T cell–mediated pneumonitis model in microbiota-free or decreasing conditions. This model may be a valuable tool for investigating the immunological mechanisms of extraintestinal disorders in patients with IBD.

Acknowledgments

We thank Dr. D. Littman for providing the mice.

Disclosures

The authors have no financial conflicts of interest.

References

1. Podolsky, D. K. 2002. Inflammatory bowel disease. *N. Engl. J. Med.* 347: 417–429.
2. Sartor, R. B. 2006. Mechanisms of disease: pathogenesis of Crohn's disease and ulcerative colitis. *Nat. Clin. Pract. Gastroenterol. Hepatol.* 3: 390–407.
3. Elson, C. O., Y. Cong, V. J. McCracken, R. A. Dimmitt, R. G. Lorenz, and C. T. Weaver. 2005. Experimental models of inflammatory bowel disease reveal innate, adaptive, and regulatory mechanisms of host dialogue with the microbiota. *Immunol. Rev.* 206: 260–276.
4. Maynard, C. L., and C. T. Weaver. 2009. Intestinal effector T cells in health and disease. *Immunity* 31: 389–400 (Review).
5. Kassiotis, G., S. Garcia, E. Simpson, and B. Stockinger. 2002. Impairment of immunological memory in the absence of MHC despite survival of memory T cells. *Nat. Immunol.* 3: 244–250.
6. Nemoto, Y., T. Kanai, K. Kameyama, T. Shinohara, N. Sakamoto, T. Totsuka, R. Okamoto, K. Tsuchiya, T. Nakamura, T. Sudo, et al. 2009. Long-lived colitogenic $CD4^+$ memory T cells residing outside the intestine participate in the perpetuation of chronic colitis. *J. Immunol.* 183: 5059–5068.
7. Nemoto, Y., T. Kanai, S. Makita, R. Okamoto, T. Totsuka, K. Takeda, and M. Watanabe. 2007. Bone marrow retaining colitogenic $CD4^+$ T cells may be a pathogenic reservoir for chronic colitis. *Gastroenterology* 132: 176–189.
8. Totsuka, T., T. Kanai, Y. Nemoto, T. Tomita, K. Tsuchiya, N. Sakamoto, R. Okamoto, and M. Watanabe. 2008. Immunosenescent colitogenic $CD4^+$ T cells convert to regulatory cells and suppress colitis. *Eur. J. Immunol.* 38: 1275–1286.
9. Baumgart, D. C., and W. J. Sandborn. 2007. Inflammatory bowel disease: clinical aspects and established and evolving therapies. *Lancet* 369: 1641–1657.
10. Clemente, J. C., L. K. Ursell, L. W. Parfrey, and R. Knight. 2012. The impact of the gut microbiota on human health: an integrative view. *Cell* 148: 1258–1270.
11. Berer, K., M. Mues, M. Koutrolos, Z. A. Rasbi, M. Boziki, C. Johner, H. Wekerle, and G. Krishnamoorthy. 2011. Commensal microbiota and myelin autoantigen cooperate to trigger autoimmune demyelination. *Nature* 479: 538–541.
12. Hwang, S. J., S. Kim, W. S. Park, and D. H. Chung. 2006. IL-4-secreting NKT cells prevent hypersensitivity pneumonitis by suppressing IFN-γ-producing neutrophils. *J. Immunol.* 177: 5258–5268.
13. Rangel-Moreno, J., D. M. Carragher, M. de la Luz Garcia-Hernandez, J. Y. Hwang, K. Kusser, L. Hartson, J. K. Kolls, S. A. Khader, and T. D. Randall. 2011. The development of inducible bronchus-associated lymphoid tissue depends on IL-17. *Nat. Immunol.* 12: 639–646.
14. Sujino, T., T. Kanai, Y. Ono, Y. Mikami, A. Hayashi, T. Doi, K. Matsuoka, T. Hisamatsu, H. Takaishi, H. Ogata, et al. 2011. Regulatory T cells suppress development of colitis, blocking differentiation of T-helper 17 into alternative T-helper 1 cells. *Gastroenterology* 141: 1014–1023.
15. Chapman, T. J., and D. J. Topham. 2010. Identification of a unique population of tissue-memory $CD4^+$ T cells in the airways after influenza infection that is dependent on the integrin VLA-1. *J. Immunol.* 184: 3841–3849.
16. Sheridan, B. S., and L. Lefrançois. 2011. Regional and mucosal memory T cells. *Nat. Immunol.* 12: 485–491 (Review).
17. Leach, M. W., A. G. Bean, S. Mauze, R. L. Coffman, and F. Powire. 1996. Inflammatory bowel disease in C.B-17 scid mice reconstituted with the CD45RBhigh subset of CD4+ T cells. *Am. J. Pathol.* 148: 1503–1515.
18. Surh, C. D., and J. Sprent. 2008. Homeostasis of naive and memory T cells. *Immunity* 29: 848–862 (Review).
19. Sakaguchi, S., N. Sakaguchi, M. Asano, M. Itoh, and M. Toda. 1995. Immunologic self-tolerance maintained by activated T cells expressing IL-2 receptor α-chains (CD25): breakdown of a single mechanism of self-tolerance causes various autoimmune diseases. *J. Immunol.* 155: 1151–1164.
20. Asano, M., M. Toda, N. Sakaguchi, and S. Sakaguchi. 1996. Autoimmune disease as a consequence of developmental abnormality of a T cell subpopulation. *J. Exp. Med.* 184: 387–396.
21. Barthlott, T., G. Kassiotis, and B. Stockinger. 2003. T cell regulation as a side effect of homeostasis and competition. *J. Exp. Med.* 197: 451–460.
22. Sprent, J., and C. D. Surh. 2002. T cell memory. *Annu. Rev. Immunol.* 20: 551–579.
23. Storch, I., D. Sachar, and S. Katz. 2003. Pulmonary manifestations of inflammatory bowel disease. *Inflamm. Bowel Dis.* 9: 104–115 (Review).

Mannan-Binding Protein, a C-Type Serum Lectin, Recognizes Primary Colorectal Carcinomas through Tumor-Associated Lewis Glycans

Motohiro Nonaka,*,† Hirotsugu Imaeda,‡ Shogo Matsumoto,* Bruce Yong Ma,*,§,¶,‖ Nobuko Kawasaki,* Eiji Mekata,# Akira Andoh,** Yasuharu Saito,†† Tohru Tani,# Yoshihide Fujiyama,‡ and Toshisuke Kawasaki*

Mannan (mannose)-binding protein (MBP) is a C-type serum lectin that plays a key role in innate immunity. MBP forms large multimers (200–600 kDa) and exhibits broad specificity for mannose, *N*-acetylglucosamine, and fucose. MBP exhibits high affinity for unique oligosaccharides that have been isolated from human colorectal carcinoma (SW1116) cells and characterized as highly fucosylated high m.w. type 1 Lewis glycans. In this study, we first demonstrated that MBP recognizes human primary colorectal carcinoma tissues through tumor-associated MBP ligands. We performed fluorescence-based histochemistry of MBP in human colorectal carcinoma tissues and showed that MBP clearly stained cancer mucosae in a Ca^{2+}-dependent manner. Coincubation with plant (*Aleuria aurantia*) lectin, but not Con A, blocked MBP staining, indicating that fucose, rather than mannose, is involved in this interaction. The expression of MBP ligands was detected in 127 of 330 patients (38.5%), whereas, most significantly, there was no expression in 69 nonmalignant tissues. The MBP-staining pattern in cancer mucosae significantly overlapped with that of Lewis b [Fucα1-2Galβ1-3(Fucα1-4)GlcNAc] staining, but the Lewis b staining in normal tissues was not associated with MBP staining. In addition, the MBP staining correlated inversely with the expression of CA19-9 Ag, and MBP stained 11 of 25 (44%) CA19-9 (sialyl Lewis a [NeuAc(α2-3)Galβ1-3(Fucα1-4)GlcNAc])$^-$ colorectal carcinoma tissues. We found a favorable prognosis in patients with MBP ligand$^+$ tumors. These results suggest that selective recognition of cancer cells by endogenous MBP seems to be associated with an antitumor effect and that tissue staining with MBP in combination with CA19-9 may serve as a novel indicator of colorectal carcinoma tissues. ***The Journal of Immunology*, 2014, 192: 1294–1301.**

Mannan (mannose)-binding protein (MBP), also known as mannan-binding lectin, is a Ca^{2+}-dependent (C-type) serum lectin that plays a key role in first-line host defense (1–4). MBP interacts with a broad spectrum of bacterial and viral infectious pathogens through its carbohydrate-recognition domain (CRD) (5–9). Binding of MBP leads to complement fixation on the surface of bacteria, blocking of viral infectivity, and opsonization of fungi before the development of a specific Ab response. MBP exhibits specificity for mannose, fucose, *N*-acetylglucosamine, glucose, and derivatives of these sugars but not for galactose and sialic acid, which are the ultimate and penultimate carbohydrate residues of most mammalian glycoproteins (10, 11). Three identical monomers of MBP (31 kDa) associate to form primary structural subunits, which assemble into larger multimers (200–600 kDa) (12). On the formation of multimers, the binding affinity of MBP for complex and multivalent ligands becomes much higher than that for monosaccharides (13). Some years ago, we found that MBP bound specifically to a number of human colorectal cell lines and exhibited potent growth inhibitory activity toward a human colorectal carcinoma cell line (SW1116) in nude mice (MBP-dependent cell-mediated cytotoxicity [MDCC]) (14). In the following studies, we isolated MBP ligand oligosaccharides using an affinity column of MBP-Sepharose 4B from an oligosaccharide mixture prepared by hydrazinolysis of pronase digests of SW1116 cells. They are large, multiantennary *N*-glycans with highly fucosylated polylactosamine-type structures having Lewis b [Fucα1-2Galβ1-3(Fucα1-4)GlcNAc] (Le^b)– Lewis a [Galβ1-3(Fucα1-4)GlcNAc] (Le^a) or tandem repeats of the Le^a structure at their nonreducing ends (15). To our knowledge, these glycans were the first endogenous oligosaccharides that showed the capability to bind to MBP with high affinity. These results led us to examine whether MBP can distinguish cancer tissues from noncancerous ones in cancer patients.

In this study, we used immunohistochemistry to detect MBP ligands on primary human colorectal tissues systematically. We demonstrated that MBP ligands were expressed in 127 of 330

*Research Center for Glycobiotechnology, Ritsumeikan University, Shiga 525-8577, Japan; †Cancer Center, Sanford-Burnham Medical Research Institute, La Jolla, CA 92037; ‡Department of Medicine, Shiga University of Medical Science, Shiga 520-2192, Japan; §School of Pharmaceutical Engineering and Life Science, Changzhou University, Jiangsu 213164, China; ¶ZonHon Biopharma Institute, Inc., Jiangsu 213022, China; ‖Department of Computer Science and Systems Engineering, Muroran Institute of Technology, Hokkaido 050-8585, Japan; #Department of Surgery, Shiga University of Medical Science, Shiga 520-2192, Japan; **Division of Mucosal Immunology, Graduate School of Medicine, Shiga University of Medical Science, Shiga 520-2192, Japan; and ††University Hospital Department of Endoscopic Diagnostics and Therapeutics, Shiga University of Medical Science, Shiga 520-2192, Japan

Received for publication October 31, 2012. Accepted for publication November 26, 2013.

This work was supported by Grants-in-Aid for Scientific Research B 20370052 (to T.K.) and C 21590543 (to B.Y.M.) and Fellowship 22-9530 (to M.N.) from the Japan Society for the Promotion of Science, Ministry of Education, Culture, Sports, Science and Technology of Japan, as well as by Core-to-Core Program-Strategic Research Networks 17005 sponsored by the Japan Society for the Promotion of Science.

Address correspondence and reprint requests to Dr. Toshisuke Kawasaki, Research Center for Glycobiotechnology, Ritsumeikan University, Nojihigashi 1-1-1, Kusatsu, Shiga 525-8577, Japan. E-mail address: tkawasak@fc.ritsumei.ac.jp

Abbreviations used in this article: AAL, *Aleuria aurantia* lectin; CEA, carcinoembryonic Ag; CI, confidence interval; CRD, carbohydrate-recognition domain; Le, Lewis; Le^a, Lewis a [Galβ1-3(Fucα1-4)GlcNAc]; Le^b, Lewis b [Fucα1-2Galβ1-3(Fucα1-4)GlcNAc]; MBP, mannan (mannose)-binding protein; MDCC, mannan-binding protein–dependent cell-mediated cytotoxicity; pAb, polyclonal Ab.

www.jimmunol.org/cgi/doi/10.4049/jimmunol.1203023

carcinoma patients (38.5%), but they were not expressed in 69 nonmalignant tissues. MBP staining correlated inversely with the expression of CA19-9 among carcinoma patients. Cox proportional hazards regression analysis demonstrated that there was a positive correlation between MBP ligand expression and favorable survival rate. These data indicate the physiological significance of endogenous MBP in colorectal carcinomas, as well as suggest that exogenous MBP is a novel tool for the diagnosis or prognosis of colorectal carcinomas.

Materials and Methods

Patients and cancer tissues

Thirty-five primary colorectal carcinoma tissue specimens including adjacent noncancerous epithelium were obtained from patients who underwent surgery or endoscopic submucosal dissection from 2007 to 2009 at Shiga University of Medical Science Hospital (mean age, 68.9 ± 10.1 y; range, 45–89 y). Informed consent was provided according to the Declaration of Helsinki. Each patient provided written informed consent, and the project was approved by the ethics committees of Ritsumeikan University and Shiga University of Medical Science. The other sets of 196 and 99 colorectal carcinoma tissue specimens were obtained from SuperBioChips Laboratories (Seoul, Korea) (mean age, 58.0 ± 11.0 y; range, 30–86 y) and US Biomax (Rockville, MD) (mean age, 59.9 ± 13.4 y; range, 29–88 y), respectively. Among them, 20 metastatic tissues were available. Survival data were available for 186 patients, and the mean follow-up time was 83.0 ± 45.7 mo (range, 1–120 mo).

Reagents and Abs

MBP was purified as previously described (16). Anti-human MBP mAb was purchased from BioPorto Diagnostics (Gentofte, Denmark). Anti-Le^a (MLS103) mAb and anti-Le^b (36A) mAb are mAbs raised against human colorectal colon cancer cell lines LS180 and SW1116, respectively. MLS103 was a kind gift from Professor S. Fukui, Kyoto Sangyo University (Kyoto, Japan) (17). 36A was prepared in our laboratory (S. Matsumoto, H. Nakao, K. Kawabata, M. Kusuda Furue, M. Nonaka, Y. Takishima, H. Toyoda, T. Taki, T. Okumura, N. Kawasaki, and T. Kawasaki, manuscript in preparation). Anti-carcinoembryonic Ag (CEA) mAb was obtained from Abcam (Cambridge, MA), and anti-sialyl Le^a (CA19-9) mAb was from Seikagaku Biobusiness (Tokyo, Japan). Anti-CD3ε polyclonal Ab (pAb) was from Santa Cruz Biotechnology (Santa Cruz, CA), anti–HLA-DR mAb and anti-CD83 mAb were from BioLegend (San Diego, CA), and anti-CD163 mAb was from eBioscience (San Diego, CA). Alexa Fluor 488 goat anti-mouse IgG pAb and TO-PRO3 were from Invitrogen-Life Technologies (Carlsbad, CA). Con A was from Sigma-Aldrich (St. Louis, MO), and *Aleuria aurantia* lectin (AAL) was from Seikagaku Biobusiness.

Histochemistry

Following deparaffinization and hydration of paraffin-embedded tissue sections, Ag retrieval was performed by steaming in citrate buffer (pH 6). After incubation in blocking buffer (TBS buffer [pH 7.6] containing 1% BSA), the sections were incubated with 2 μg/ml human MBP in the presence of 5 mM $CaCl_2$ or EDTA at room temperature for 1 h and then washed with TBS buffer [pH 7.6] containing $CaCl_2$ or EDTA. Following incubation with 2.5 μg/ml anti-MBP mAb for 1 h, the slides were washed, incubated with Alexa Fluor 488–conjugated secondary pAb and TO-PRO3 for 1 h, and washed in the presence of $CaCl_2$. For competitive-binding assays, slides were preincubated in blocking buffer containing 5 mM $CaCl_2$ or 10 mM EDTA, 5 mM $CaCl_2$ plus 100 μM Con A, or 5 mM $CaCl_2$ plus 100 μM AAL for 30 min; purified MBP was added, and the slides were incubated together with each of the competitors for 1 h. For tumor-infiltration analyses, slides were incubated with anti-CD3ε pAb or with anti–HLA-DR mAb for 30 min, followed by incubation with Alexa Fluor–conjugated secondary pAb. For double staining of MBP and Le glycans, slides were incubated with anti-MBP mAb and anti-Le^a mAb or anti-Le^b mAb for 1 h, followed by incubation with Alexa Fluor–conjugated secondary pAb. For immune infiltration, slides were coincubated with anti–HLA-DR mAb and anti-CD83 mAb, anti-CD163 mAb or anti-MBP mAb for 1 h, followed by incubation with Alexa Fluor–conjugated secondary pAb. The tissue localization of MBP ligand, Le^a, Le^b, CD3, CD83, CD163, and HLA-DR were visualized by laser confocal microscopy (FluoView 1000; Olympus, Tokyo, Japan). For comparative histological analysis, serial tissue sections were subjected to H&E staining, according to standard procedures, and observed under a light microscope.

Immunohistochemical assessment

All tissue sections were evaluated in a coded manner without knowledge of the clinical and pathological parameters. By taking into account both the staining intensity and the percentage of the tumor cut surface area, the total intensity for MBP staining, anti-CD3 pAb, or anti–HLA-DR mAb was evaluated as negative, 0; weak, 1; moderate, 2; or strong, 3. Carcinoma samples exhibiting significant staining intensity (intensity 2 and 3) were classified as positive expressers of MBP ligands, CD3, or HLA-DR, and the remaining samples were classified as negative expressers of MBP ligands. Assessment was performed by five independent investigators (M. Nonaka, S. Matsumoto, H. Nakao, N. Kawasaki, and T. Kawasaki).

Statistical analysis

The relationship between the expression of MBP ligands and clinicopathological variables was statistically evaluated by means of a χ^2 test with GraphPad Prism software (version 5.0d, GraphPad, La Jolla, CA). Patients were followed up, the survival curves were estimated by the Kaplan–Meier method, and the resulting curves were compared using the log-rank test. Statistical analyses with multivariate Cox proportional hazards models were performed by EZR software (Saitama Medical Center, Jichi Medical University) (18). To extract a final model of the variables that show a significantly independent relationship with survival, variables were eliminated by stepwise backward selection after including variables (gender, tumor size, nodal status, metastasis, tumor stage, histological differentiation, and MBP ligand positivity) in an initial model. In a stepwise backward-selection procedure, a p value < 0.05 was considered statistically significant.

Results

MBP recognizes cancer cells of human primary colorectal carcinoma

To determine whether MBP ligands are expressed on human primary colorectal carcinomas, we performed MBP histochemistry using the three-step staining protocol described in *Materials and Methods*. Fig. 1A shows a well-differentiated adenocarcinoma of the sigmoid colon that includes adjacent noncancerous mucosa. H&E staining showed that, although the epithelium of the noncancerous mucosa formed straight tubular crypts arranged in parallel, the cancer mucosa showed marked cellular pleomorphism, loss of nuclear polarity, and stratification of nuclei. MBP clearly stained cancer mucosae but not noncancerous mucosae, and a Ca^{2+} chelator, EDTA, abolished the staining (Fig. 1B–D), indicating that the recognition was mediated by the CRD of MBP. This staining was not detected on control treatment without primary incubation with MBP (data not shown).

We examined tissues from a total of 330 patients with adenocarcinomas or mucinous carcinomas. We found that 127 of 330 cases (38.5%) were positive for MBP staining. In contrast, the expression of MBP ligands was not detected in any of the 69 nonmalignant colon tissues (Fig. 2A, 2B). We detected three types of expression patterns among the tumor specimens: intense expression on the apical surface (Fig. 2C), diffuse cytoplasm expression of epithelial cells in adenocarcinomas (Fig. 2D), and mucus expression within malignant glands in mucinous carcinomas (Fig. 2E, 2F). Taken together, these results indicate that MBP can discriminate cancer regions from surrounding noncancerous regions. In other words, MBP ligands are expressed on cancer tissues of human primary colorectal carcinoma mucosae.

Fucose residues are associated with tumor recognition by MBP

Although MBP preferentially binds to high-mannose–type glycans or fucose-containing type-1 Lewis (Le; Le^a/Le^b) glycans expressed on a broad spectrum of foreign pathogens, only the fucose expression was upregulated in most studies on colorectal carcinomas (19–21). To determine whether a fucose moiety mediates the interaction between MBP and cancer tissues, we performed MBP histochemistry in the presence of a plant lectin: Con A or AAL. Fig. 3A shows that Con A, which exhibits high affinity for high-mannose–type glycans,

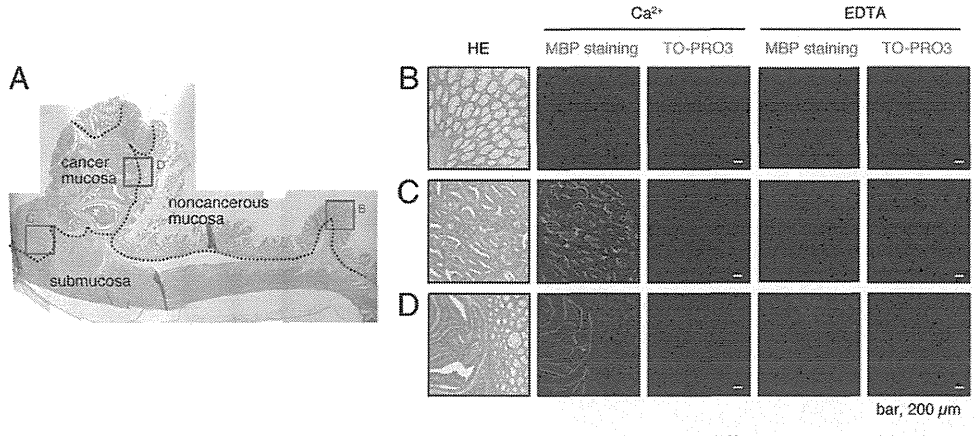

FIGURE 1. MBP specifically recognizes primary colorectal carcinoma cells. (**A**) H&E-stained well-differentiated sigmoid colon adenocarcinoma tissue with adjacent noncancerous mucosa and submucosa. MBP-stained noncancerous mucosa (**B**), cancer mucosa (**C**), and the border region (**D**). Each stained region is indicated by a red square in (A). Histochemistry with MBP (green) in the presence of 5 mM Ca^{2+} or EDTA was performed using the three-step staining protocol described in *Materials and Methods*. The images were obtained with a confocal laser microscope. TO-PRO3 (blue, pseudo-color) was used for counter-staining.

showed no inhibitory effect. In contrast, fucose-binding lectin AAL blocked this interaction. This inhibition was detected in most (15 of 16) tumor cases (Fig. 3B), indicating that fucose residues are involved in MBP recognition in primary colorectal carcinoma cells. These results were completely consistent with the binding properties of MBP to a human colon carcinoma cell line, SW1116, as described before (15).

MBP recognizes colorectal tumor–derived Le^{b+} glycans

As an extension of our previous studies on SW1116 cells, we investigated whether α1,2-fucosylated type-1 Le (Le^b-type) glycans are associated with the expression of MBP ligands on clinical samples by double staining with MBP and anti-Le^a/Le^b mAb. The anti-Le^a mAb, MLS 103, and the anti-Le^b mAb, 36A (see *Materials and Methods*), used in this study are specifically reactive with Le^a and Le^b oligosaccharides, respectively, as examined using the oligosaccharide microarray method of Fukui et al. (22). We demonstrated that the expression of Le^a glycans showed little correlation with MBP staining (Fig. 4A). In contrast, anti-Le^b mAb stained 15 of 16 (93.8%) cancer tissue specimens that were positive for MBP staining. Moreover, the Le^b expression patterns in five of these cases significantly overlapped with the patterns of MBP staining (Fig. 4A). However, Le^b glycans is commonly known as a blood-type Ag in normal (noncancerous) individuals, and anti-Le^b Abs strongly stained the goblet cells of some noncancerous colon tissues, as reported previously (23–25). In addition, it should be noted that none of these Le^{b+} glycans in the noncancerous tissues was costained with MBP, even though those Le^{b+} glycans in the cancer tissues from the same patients were extensively costained with MBP (Fig. 4B). Taken together, these findings indicate that tumor-associated anti-Le^{b+} glycan Ags are distinct from the conventional blood group Le^b Ags (i.e., the conventional Le^b tetrasaccharide epitope is a necessary component but is not sufficient for the recognition by MBP, and some other neighboring structures should be essential for the high-affinity binding to MBP, this being consistent with our previously

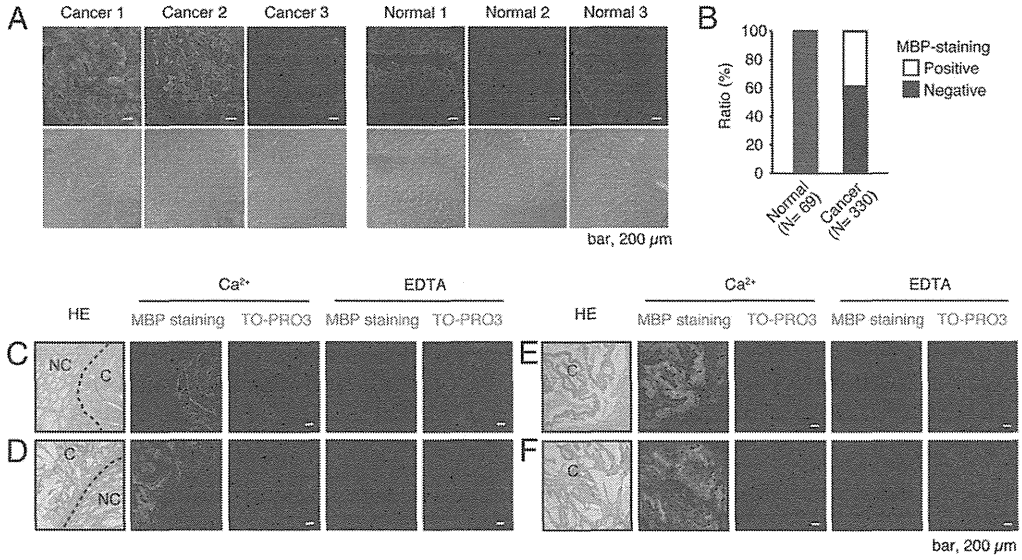

FIGURE 2. MBP shows a heterogeneous staining pattern in colorectal carcinoma tissues. (**A**) Representative image of MBP staining in 330 colorectal carcinoma and 69 normal colon tissues. Images in Cancer 1 and 2 show MBP ligand$^+$ tumor. Cancer 3 is MBP ligand$^-$. (**B**) Ratio of cases staining positive for MBP. Of note, 127 of 330 (38.5%) colorectal carcinoma tissues were stained by MBP, whereas 0 of 69 normal colon tissues was stained. MBP-staining patterns in a well-differentiated adenocarcinoma (**C**), a moderately differentiated adenocarcinoma (**D**), and a mucinous carcinoma (**E**, **F**). C, Cancer tissue; NC, noncancerous tissue.